2021 43rd Annual International Conference of the
IEEE Engineering in Medicine & Biology Society (EMBC)
Oct 31 - Nov 4, 2021. Virtual Conference

Fast Individualized High-resolution Electric Field Modeling for Computational TMS Neuronavigation*

Mohammad Daneshzand, *Member, IEEE*, Sergey N. Makarov, *Member, IEEE*, Lucia I. Navarro de Lara, and Aapo Nummenmaa

Abstract— **Transcranial Magnetic Stimulation (TMS) is a non-invasive method for safe and painless activation of cortical neurons. On-line visualization of the induced Electric field (E-field) has the potential to improve quantitative targeting and dosing of stimulation, however present commercially available systems are limited by simplified approximations of the anatomy. Here, we developed a near real-time method to accurately approximate the induced E-field of a freely moving TMS coil with an individualized high-resolution head model. We use a set of magnetic dipoles around the head to approximate the total E-field of a moving TMS coil. First, we match the incident field of the dipole basis set with the incident E-field of the moving coil. Then, based on the principle of superposition and uniqueness of the solutions, we apply same basis coefficients to the total E-field of the basis set. The computed E-fields results show high similarity with an established TMS solver both in terms of the amplitude and the spatial distribution patterns. The proposed method enables rapid visualization of the E-field with ~100 ms of computation time enabling interactive planning, targeting, dosing and coil positioning tasks for TMS neuronavigation.**

I. Introduction

Transcranial Magnetic Stimulation (TMS) combined with a near real-time display of the induced E-field in neuronavigation systems has the potential to improve the therapeutic effects of stimulation [1]. Moreover, clinical TMS protocols require several daily stimulation sessions to accumulate the effects. Thus, we need a way to reliably target TMS to the correct brain area(s) in a consistent and repeatable manner. The computational modeling of the E-field based on the individual brain anatomy can be used to visualize stimulated region or the 'hot spot' and to improve the targeting and dosing of TMS [1], [2]. However, present commercial neuronavigation systems are limited to approximations of the total E-field based on highly simplified models of the anatomy. While these models are computationally efficient, they do not account for individual skull shape and the complexity intracranial tissue geometry [3]–[5].

Several methods have been proposed for E-field calculations using high resolution head models [6], [7]. The combination of a Boundary Element Model with Fast Multilevel Multipole acceleration (BEM-FMM) [6] as well as volumetric meshing based on Finite Element Method (FEM) [8] produce accurate estimates of the intracranial fields. However, these methods are not fast enough to keep up with the 10-15 Hz frame rate of coil movements captured in the neuronavigation systems. Recent approaches have suggested utilizing GPUs [9] and Convolutional Neural Networks (CNNs) [7] to accelerate the computations. For the GPU-based method, scalability to high resolution models remains a challenge while generalizability across MRI scanners and subject populations requires more investigation.

Here we present a novel pipeline for near real-time computation and visualization of the TMS induced E-fields for an arbitrary coil type based on the Magnetic Stimulation Profile (MSP) approach [10]. The MSP is based on a set of magnetic dipoles placed on a closed surface surrounding the scalp for efficient precomputation the E-fields. For these pre-computations, we utilize the BEM-FMM approach that is state-of-the-art in terms of accuracy and speed for solving the total E-field influenced by the conductivity boundaries [6], [11]. The key advantage is that the MSP of the subject needs to be calculated and stored only once and it enables a highly efficient implementation of near real-time E-field estimation based on the tracking data of the coil position/orientation. The position and orientation of the coil is streamed from a commercial TMS navigation software (LOCALITE GmbH, Bonn, Germany) into MATLAB where the near real-time calculation/visualization is performed.

This paper is organized as follows: in section II we outline the mathematical concepts of BEM-FMM for the dipole-based MSP pre-calculations along with the near real-time E-field calculation step. In section III, we describe the main new contribution of this article that is the near real-time implementation of the proposed method and demonstrate an experimental application of the dipole-based MSP with motor cortex mapping of a healthy volunteer subject. Finally, we 'cross-validate' the E-field based estimates by comparing the motor threshold results across two TMS coil types. In section IV, we discuss the potential applications and future improvements of the method.

II. Proposed Method

The MSP-based E-field computation consists of a pre-processing and a near real-time step [10]. In the pre-processing step, the incident and the total E-fields of the magnetic dipoles are calculated and stored. The incident E-

* Research supported by NIH R00EB015445, R01MH111829, P41EB030006 and R21MH116484 grants.

M. Daneshzand, L. I. Navarro de Lara, and A. Nummenmaa are with the Athinoula A. Martinos Center for Biomedical Imaging, Department of Radiology, Harvard Medical School and Massachusetts General Hospital, Charlestown, MA, 02129, USA (phone: +1 617-724-9989; email: {mdaneshzand, lnavarrodelara, anummenmaa}@mgh.harvard.edu)

S. Makarov is with the Athinoula A. Martinos Center for Biomedical Imaging, Department of Radiology, Harvard Medical School, Massachusetts General Hospital and Department of Electrical and Computer Engineering, Worcester Polytechnic Institute, Worcester, MA, 01609, USA (email: makarov@wpi.edu)

fields from the dipole basis set can be used to match the incident E-field of the actual TMS coil, providing a set of dipole coefficients. The total E-field of a TMS coil only depends on the incident E-field of the coil and the geometry of tissue conductivity boundaries [6]. Hence, based on linear superposition the total E-field of the coil can be obtained by applying the matching coefficients to the total E-field of the dipole basis set [10]. This enables the near real-time step to be executed computationally extremely efficiently. The BEM tissue compartments (*e.g.,* skin, skull, cerebrospinal fluid, grey and white matter surfaces) are assumed to have an homogenous conductivity within each surface [12], [13].

A. Pre-Processing Step

First, we position 1500 magnetic dipoles on a fictitious surface covering the head model at 500 spatial locations (each location has three orthogonal dipoles) as shown in Figure 1 a.

The incident field $\boldsymbol{E^{inc}}$ of the dipole in free space follows the Faraday's law of induction in the form

$$\boldsymbol{E^{inc}} = -\partial A/\partial t \quad (1)$$

To calculate the secondary E-fields from each individual dipole, the surface conductivity boundaries are discretized into small triangular facets with centers c_i, normal vectors n_i and areas A_i [6]. The charge density at every triangle is obtained by an iterative solution of an integral BEM equation:

$$\rho_{i,n} = 2\varepsilon_0 \frac{\sigma_{in}-\sigma_{out}}{\sigma_{in}+\sigma_{out}} \frac{\mathrm{n}}{A_i} \cdot \int_{t_i} \{\boldsymbol{E^s_{n-1}}(c_i) + \boldsymbol{E^{inc}}(c_i)\} dr \quad (2)$$

where $\sigma_{in}, \sigma_{out}$ are in the conductivities at the interface of any two compartments. The secondary E-field is computed from the known charge distribution at the previous iteration:

$$\boldsymbol{E^s_{n-1}}(c_i) = -\sum_{j=1}^{N} \frac{A_j \rho_{j,\,n-1}}{4\pi\varepsilon_0} \frac{c_j - c_i}{|c_i - c_j|^3} \quad (3)$$

The total E-field $\boldsymbol{E^{tot}}$ is calculated as the summation of the incident and secondary E-fields. The pre-processing step required 5.7 hours in this study but only needs to run once per subject [10]. The incident and total E-fields for the full dipole basis set on the desired surfaces are stored as $\boldsymbol{E^{inc}}$ and $\boldsymbol{E^{tot}}$, respectively, and are utilized in near real-time TMS coil induced E-field calculation.

B. Near real-time step

Each row of the matrix $\boldsymbol{A_{inc}}$ corresponds to the incident field from a dipole computed at a user-specified matching surface (*e.g.,* white matter). Now, given an incident field pattern $\boldsymbol{S_{inc}}$ on the surface, we can find the best matching basis coefficients m_{LS} in the least square sense by regularized pseudoinverse:

$$W = \boldsymbol{A_{inc}^T}\left(\boldsymbol{A_{inc}}\boldsymbol{A_{inc}^T} + \lambda I\right)^{-1} \quad (4)$$

$$m_{LS} = W\boldsymbol{S_{inc}} \quad (5)$$

The total E-field on the surface is then obtained by a matrix multiplication:

$$\boldsymbol{S_{tot}} = \boldsymbol{A_{tot}} m_{LS} \quad (6)$$

The problem has therefore been cast into a convenient matrix formalism through the MSP that is straightforward to implement for near real-time computations. Figure 1 b shows a commercially available Cool B-35 coil (MagVenture, Farum, Denmark) placed tangentially on the skin. We used the BEM-FMM Equations (1-3) [6], [11] to calculate the ground truth E-field (Figure 1 d). The dipole amplitudes are optimized to match the incident field of the coil by Equation (4-5) as shown in Figure 1 c and the matching coefficients are used to calculate the total E-field based on Equation (6) (Figure 1 e). The total E-field on the white matter surface computed with the proposed MSP approach matches the ground truth BEM-FMM results both terms of intensity and spatial distribution [10].

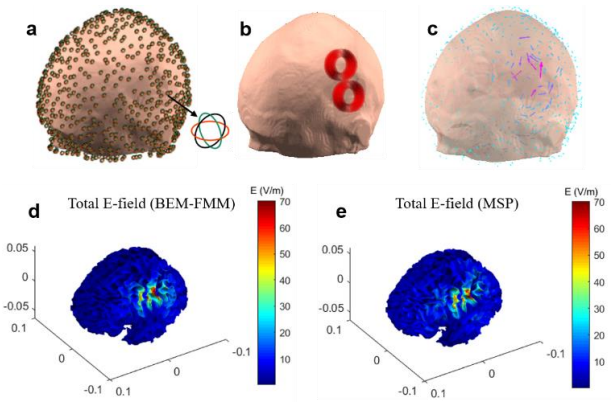

Fig. 1. TMS-induced E-field calculation based on the MSP approach. A set of orthogonal dipoles placed at 2mm distance from the skin surface (a) are used for modeling the E-fields of a Cool B-35 TMS coil (b). There are three orthogonal dipoles at each location (a). The amplitudes of the dipole basis function for the approximation shown in (c) closely match the E-field pattern of the coil. The ground truth E-field distribution obtained from the BEM-FMM method (d) is compared with the MSP approach (e).

C. Accuracy Metrics

To compare the accuracy of the E-fields generated by the MSP approach with the ground truth BEM-FMM we used the Correlation Coefficients (CC) and Relative Error (RE) metrics [9]. The CC metric quantifies the similarity in the E-fields spatial distribution as:

$$CC = \frac{(E_r - \bar{E_r}).(E_M - \bar{E_M})}{|E_r - \bar{E_r}||E_M - \bar{E_M}|} \quad (7)$$

Where E_r and E_M represent the total E-field vectors generated by the BEM-FMM and MSP approaches, respectively. The RE quantifies the amplitude difference between the two methods by:

$$RE = \frac{|E_r - E_M|}{|E_r|} \quad (8)$$

D. E-field based computational TMS neuronavigation

In order to continuously record the coil position with respect to the subject's head, we used an optical tracking camera (Polaris Spectra, NDI, Northern Digital Inc, Canada) in combination with a commercially available TMS navigation system (LOCALITE Gmbh, Bonn, Germany). The navigation system updates the coil position data at a 10-15 Hz frame rate allowing a smooth visualization of arbitrary coil movements. The coil position data is read from the navigation system computer by JavaScript Object Notation

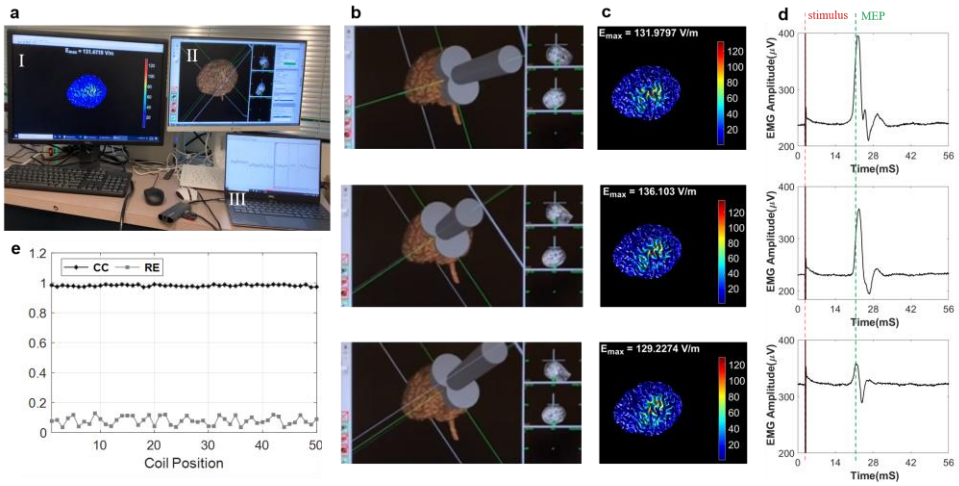

Fig. 2. E-field based Navigation pipeline. (a) The experiment setup consists of (I) the Localite navigator system that tracks the coil position with respect to the head using reflectors, (II) the E-field calculation system and (III) the EMG recording laptop. The coil can be placed at the desired motor cortex target with the navigation software (shown in b) or based on the E-field display (shown in c). Once the TMS pulses are delivered at the target the EMG muscle response is displayed (d) and evaluated for accurate detection of the resting motor threshold. (e) Accuracy metrics across 50 coil positions.

(JSON) interface and streamed to another computer where the near real-time E-field calculation step is implemented. For the near real-time computations, we used MATLAB 2019a on an Intel Xeon CPU ES-2360, 2.4 GHz with 128 GB of memory. The near real-time E-field visualization was used in an experimental setup to determine the cortical hotspot and to find the E-field intensity that corresponds to the subject's resting Motor Threshold (rMT) [14]. The rMT varies between individuals and much of this variability has been attributed to geometrical differences in brain and skull [15]. Here, we aimed to enable normalizing the targeting and dosing of stimulation with respect to the physical variability, to deliver pre-determined E-field intensity to the desired brain structure with best possible accuracy. When the TMS hot spot location was identified, we used two different coils with different diameters and depth penetration profiles [16] (MagPro C-B60 and Cool-B35) to cross-validate the predicted E-field intensities at the target with the coil position locked to the optimal one. To obtain quantitative rMT values, individual pulses were delivered while recording the Electromyography (EMG) muscle responses. Informed consent was obtained from the human subject in accordance with the study protocol approved by the IRB at Massachusetts General Hospital.

III. Results

Figure 2 a shows the experimental setup for the near real-time E-field based navigation. The TMS coil position is streamed from the Localite navigation system (Figure 2 b) into MATLAB using an ethernet connection and the TCP/IP protocol provided by the Instrument Control Toolbox (MathWorks, Inc). The E-field is then calculated for any coil position with the MSP approach (Figure 2 c). The coil position was adjusted to maximize the E-field intensity along the motor cortex at pre-central gyrus as shown in Figure 2 c. The operator sent single TMS pulses and the corresponding EMG responses were recorded. As shown in Figure 2 d, the typical EMG responses of the hand first dorsal interosseus (FDI) muscle exceed 50 μV peak-to-peak in amplitude with a 20 ms latency[17]. Near real-time E-field computation takes about 100-180 ms depending on the density of the triangulated surface meshes, which gives the theoretical frame rate of 5-10 Hz. Here the computation was done on the white matter surface with 60K vertices for incident field matching and visualization of the total E-field. The current Localite TMS navigator can track the coil position data at 5-15 Hz rates, so our present performance matches this well. Therefore, our computational performance explicitly shows that the proposed system can meet or exceed a >10 Hz frame rate. The prototype illustrated in Figure 2 a operates at around 2 Hz due to a delay of ~200 msec for streaming the data from Localite using a TCP/IP protocol as well as an additional time of 150 msec for rendering the E-field using standard built-in MATLAB functions. Memory-wise, the entire precomputation step with a model of ~750k elements takes ~ 8 GB of memory with 1500 basis functions.

Figure 2 e depicts the CC and RE comparisons of the MSP approach with the BEM-FMM for 50 coil positions. Generally, the CC metric is around 0.98 among all coil positions, suggesting that the E-field patterns produced by the MPS approach are spatially highly consistent with the BEM-FMM results. The RE metrics suggests a small difference of 3-12 % in the E-field amplitudes, however in average the RE is around 7% and the error drops drastically whenever the coil is placed tangentially to the scalp [10].

The motor cortical target is found using the standard motor mapping assisted with the near real-time estimated E-fields as shown in Figure 3 a. After identifying the hot spot, we used two different coils (MagPro C-B60 and Cool-B35) with different diameters and depth penetration profiles [16] to determine the rMT in the units of the maximal stimulator output (MSO). Using these values, we predicted E-field intensities at the target with the coil position locked to the optimal one (Figure 3 b and d). The required pulse intensity for the coil C-B60 was 76 $\frac{A}{\mu S}$ which corresponds to 41% of the MSO. For the more focal Cool B-35 coil the motor cortex threshold was at 93 $\frac{A}{\mu S}$ (65% MSO).

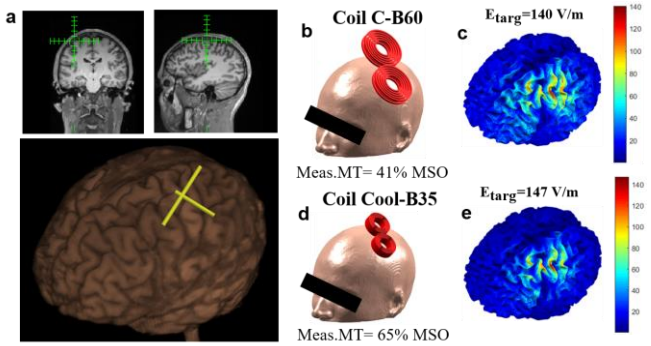

Fig. 3. Computationally determined coil position to optimally stimulate the target (a) for two coils and empirical assessment of the computational prediction of the MT between two coils (b-d). (c) and (e) show the corresponding calculated E-fields for each coil.

Finally, in Figure 3 c and e we show robust agreement in the total E-field intensities at motor threshold for the two coils. This experiment also illustrates a significant benefit of the MSP approach as the basis set is independent of the coil type and can be coupled with any TMS coil with the incident field matching process explained by Equation (5) [10].

IV. Conclusion

The most significant source of variability in targeting TMS lies in the consistent positioning of the coil relative to the head which can be reduced by using a TMS navigation system[2]. However, with a conventional navigation system the actual stimulation intensity at the intracranial target and the surrounding regions remains unknown. Therefore, when approaching TMS targeting quantitatively, the most critical task is to computationally estimate the intracranial distribution of the TMS-induced E-field intensity and determining the activated areas. To test the additional accuracy offered by the real-time computations, we plan to carry out experiments where an operator will adjust the position of the coil and stimulation intensity using the interactive E-field display only. In such case, the 'ground truth hot spot' may be defined by an exhaustive motor mapping performed by another independent operator and the theoretical intensity can be determined by the cortical E-field at the target. Furthermore, quantitative rMT values can be measured by sending individual pulses while recording the EMG muscle responses either by using conventional navigation or 'E-field enhanced' computational system to compare the consistency across trials. In conclusion, the proposed MSP approach enables TMS navigation at an unprecedented spatial precision. This ensures that the intended cortical target is stimulated with the desired E-field intensity. Additionally, the interactive MSP based neuronavigation can be used for presurgical motor mapping as well as providing a tool for offline planning and targeting of TMS sessions. In future, we expect to further increase speed to the 10-20 Hz range by upgrading the CPU, minimizing the delay in receiving the tracking data and overall code optimization including custom built rendering functions. We will also investigate the possibility of visualizing the E-field data on the Localite navigator online display.

References

[1] L. D. Gugino *et al.*, "Transcranial magnetic stimulation coregistered with MRI: a comparison of a guided versus blind stimulation technique and its effect on evoked compound muscle action potentials," *Clin. Neurophysiol.*, vol. 112, no. 10, pp. 1781–1792, 2001.

[2] J. Ruohonen and J. Karhu, "Navigated transcranial magnetic stimulation," *Neurophysiol. Clin. Neurophysiol.*, vol. 40, no. 1, pp. 7–17, 2010.

[3] M. Chen and D. J. Mogul, "A structurally detailed finite element human head model for simulation of transcranial magnetic stimulation.," *J. Neurosci. Methods*, vol. 179, no. 1, pp. 111–120, Apr. 2009, doi: 10.1016/j.jneumeth.2009.01.010.

[4] I. Laakso and A. Hirata, "Fast multigrid-based computation of the induced electric field for transcranial magnetic stimulation.," *Phys. Med. Biol.*, vol. 57, no. 23, pp. 7753–7765, Dec. 2012, doi: 10.1088/0031-9155/57/23/7753.

[5] F. S. Salinas, J. L. Lancaster, and P. T. Fox, "3D modeling of the total electric field induced by transcranial magnetic stimulation using the boundary element method," *Phys. Med. \& Biol.*, vol. 54, no. 12, p. 3631, 2009.

[6] S. N. Makarov, G. M. Noetscher, T. Raij, and A. Nummenmaa, "A Quasi-Static Boundary Element Approach With Fast Multipole Acceleration for High-Resolution Bioelectromagnetic Models," *IEEE Trans. Biomed. Eng.*, vol. 65, no. 12, pp. 2675–2683, 2018, doi: 10.1109/TBME.2018.2813261.

[7] T. Yokota *et al.*, "Real-time estimation of electric fields induced by transcranial magnetic stimulation with deep neural networks.," *Brain Stimul.*, vol. 12, no. 6, pp. 1500–1507, 2019, doi: 10.1016/j.brs.2019.06.015.

[8] G. B. Saturnino, K. H. Madsen, and A. Thielscher, "Electric field simulations for transcranial brain stimulation using FEM: an efficient implementation and error analysis," *J. Neural Eng.*, vol. 16, no. 6, p. 66032, 2019.

[9] M. Stenroos and L. M. Koponen, "Real-time computation of the TMS-induced electric field in a realistic head model," *Neuroimage*, vol. 203, no. August, p. 116159, 2019, doi: 10.1016/j.neuroimage.2019.116159.

[10] M. Daneshzand *et al.*, "Rapid computation of TMS-induced E-fields using a dipole-based magnetic stimulation profile approach," *Neuroimage*, 2021, https://doi.org/10.1016/j.neuroimage.2021.118097

[11] S. N. Makarov, W. A. Wartman, M. Daneshzand, and K. Fujimoto, "A Software Toolkit for TMS Electric-Field Modeling with Boundary Element Fast Multipole Method : An Efficient MATLAB Implementation," pp. 1–37, 2020.

[12] G. B. Saturnino, O. Puonti, J. D. Nielsen, D. Antonenko, K. H. Madsen, and A. Thielscher, "Simnibs 2.1: A comprehensive pipeline for individualized electric field modelling for transcranial brain stimulation," in *Brain and Human Body Modeling*, Springer, Cham, 2019, pp. 3–25.

[13] A. T. Htet, E. H. Burnham, G. M. Noetscher, D. N. Pham, A. Nummenmaa, and S. N. Makarov, "Collection of CAD human head models for electromagnetic simulations and their applications," *Biomed. Phys. Eng. Express*, vol. 5, no. 6, 2019, doi: 10.1088/2057-1976/ab4c76.

[14] K. Weise, O. Numssen, A. Thielscher, G. Hartwigsen, and T. R. Knösche, "A novel approach to localize cortical TMS effects," *Neuroimage*, vol. 209, p. 116486, 2020.

[15] A. Opitz, W. Legon, A. Rowlands, W. K. Bickel, W. Paulus, and W. J. Tyler, "Physiological observations validate finite element models for estimating subject-specific electric field distributions induced by transcranial magnetic stimulation of the human motor cortex," *Neuroimage*, vol. 81, pp. 253–264, 2013.

[16] Z.-D. Deng, S. H. Lisanby, and A. V Peterchev, "Electric field depth--focality tradeoff in transcranial magnetic stimulation: simulation comparison of 50 coil designs," *Brain Stimul.*, vol. 6, no. 1, pp. 1–13, 2013.

[17] P. M. Rossini *et al.*, "Non-invasive electrical and magnetic stimulation of the brain, spinal cord, roots and peripheral nerves: basic principles and procedures for routine clinical and research application. An updated report from an IFCN Committee," *Clin. Neurophysiol.*, vol. 126, no. 6, pp. 1071–1107, 2015.